CORE
Metadata, citation and similar papers at core.ac.uk
Provided by University of Tennessee, Knoxville: Trace

University of Tennessee, Knoxville
Trace: Tennessee Research and Creative Exchange

Masters Theses

Graduate School

8-2012

A Memory Controller for FPGA Applications

Bryan Jacob Hunter
bhunter6@utk.edu

Recommended Citation
Hunter, Bryan Jacob, "A Memory Controller for FPGA Applications. " Master's Thesis, University of Tennessee, 2012.
https://trace.tennessee.edu/utk_gradthes/1305

This Thesis is brought to you for free and open access by the Graduate School at Trace: Tennessee Research and Creative Exchange. It has been accepted for inclusion in Masters Theses by an authorized administrator of Trace: Tennessee Research and Creative Exchange. For more information, please contact trace@utk.edu.

To the Graduate Council:

I am submitting herewith a thesis written by Bryan Jacob Hunter entitled "A Memory Controller for FPGA Applications." I have examined the final electronic copy of this thesis for form and content and recommend that it be accepted in partial fulfillment of the requirements for the degree of Master of Science, with a major in Computer Engineering.

Gregory D. Peterson, Major Professor

We have read this thesis and recommend its acceptance:

Gregory D. Peterson, Hairong Qi, Nathanael Paul

Accepted for the Council:
Dixie L. Thompson

Vice Provost and Dean of the Graduate School

(Original signatures are on file with official student records.)

To the Graduate Council:

I am submitting herewith a thesis written by Bryan Jacob Hunter entitled "A Memory Controller for FPGA Applications." I have examined the final paper copy of this thesis for form and content and recommend that it be accepted in partial fulfillment of the requirements for the degree of Master of Science, with a major in Computer Engineering.

Dr. Gregory D. Peterson, Major Professor

We have read this thesis
and recommend its acceptance:

Dr. Hairong Qi

Dr. Nathanael Paul

Accepted for the Council:

Carolyn R. Hodges

Vice Provost and Dean of the Graduate School

To the Graduate Council:

I am submitting herewith a thesis written by Bryan Jacob Hunter entitled "A Memory Controller for FPGA Applications." I have examined the final electronic copy of this thesis for form and content and recommend that it be accepted in partial fulfillment of the requirements for the degree of Master of Science, with a major in Computer Engineering.

Dr. Gregory D. Peterson, Major Professor

We have read this thesis
and recommend its acceptance:

Dr. Hairong Qi

Dr. Nathanael Paul

Accepted for the Council:

Carolyn R. Hodges

Vice Provost and Dean of the Graduate School

(Original signatures are on file with official student records.)

A Memory Controller for FPGA Applications

A Thesis Presented for
The Master of Science
Degree
The University of Tennessee, Knoxville

Bryan Jacob Hunter

August 2012

© by Bryan Jacob Hunter, 2012
All Rights Reserved.

Acknowledgements

I would like to thank everyone that has supported me through the years. I would name you, but then this page might be longer than my thesis.

Abstract

As designers and researchers strive to achieve higher performance, field-programmable gate arrays (FPGAs) become an increasingly attractive solution. As coprocessors, FPGAs can provide application specific acceleration that cannot be matched by modern processors. Most of these applications will make use of large data sets, so achieving acceleration will require a capable interface to this data. The research in this thesis describes the design of a memory controller that is both efficient and flexible for FPGA applications requiring floating point operations. In particular, the benefits of certain design choices are explored, including: scalability, memory caching, and configurable precision. Results are given to prove the controller's effectiveness and to compare various design trade-offs.

Contents

List of Tables **vii**

List of Figures **viii**

1 Introduction and Motivation **1**

2 Hardware Design **3**

2.1 Platform 3

2.2 FPGA Design 4

2.2.1 Top Level Module 5

2.2.2 Memory Controller 7

2.2.3 User Design 16

3 Software Design **21**

3.1 Software and FPGA Interface 21

3.2 Program Overview 23

4 Implementation and Results **25**

4.1 Hardware Implementation and Performance Models 25

4.2 Software Implementation 30

4.3 Overall Performance Model 32

4.4 Expected Results 32

4.5 Results 38

5 Discussion 44

6 Conclusion 46

7 Related Work 47

Bibliography 54

Vita 59

List of Tables

2.1 Specs for Altera's Floating Point Megafunctions. 19

3.1 Functions from PROC API used in design. 22

4.1 Number of floating-point units in design that can fit into the FPGA with given precision. 26

4.2 Fitter Summary provided by Quartus II Software. 27

4.3 Parameters used for different precisions. 33

List of Figures

2.1 PROCStar III Board. 4

2.2 System Design Overview. 5

2.3 Toggle signal that gives memory control to Hardware or Software. . . 6

2.4 Timing Diagram for PROCMultiport IP for Reading and Writing to Memory [12]. 8

2.5 Conversion Process to and from SDRAM. 9

2.6 Conversion from Double Precision to 24 bit precision with exponent width 6 and mantissa width 17. 11

2.7 Conversion from 24 bit precision with exponent width 6 and mantissa width 17 to Double Precision. 12

2.8 Conversion from 24 bit precision with exponent width 6 and mantissa width 17 to Double Precision. 12

2.9 Iteration of matrix multiply. 17

2.10 Hardware view of one iteration of matrix multiply. 18

4.1 Matrix multiply divided into blocked matrix multiply and then vector multiply. 28

4.2 Mean Squared Error vs Matrix Size for different precisions of matrix multiplication. 38

4.3 Execution Times vs Matrix Size for FPGA (using all 4 FPGAs) and CPU implementations. 39

4.4 Speedup of matrix multiplication on FPGA compared to double precision matrix multiplication performed on CPU. 40
4.5 Execution Times vs Matrix Size for matrix multiplication on FPGA with caching and no caching. 40
4.6 Speedup of using caching compared to not using caching on FPGA. . 41
4.7 Scalability for single precision. 42
4.8 Speedup for single precision over using 1 FPGA. 42
4.9 Scalability for double precision. 43
4.10 Speedup for double precision over using 1 FPGA. 43

7.1 Authentication with Traditional Two-factor Hardware Security Tokens. [30] 49
7.2 Secure Identity Management through Hardware-enforced Security Policies. 50
7.3 Design of Prototype. 53

Chapter 1

Introduction and Motivation

A field-programmable gate array (FPGA) is an integrated circuit that consists of logic blocks of digital circuitry that can be programmed as hardware. Rather than being restricted to only certain hardware functions, as you are with application-specific integrated circuits (ASICs), an FPGA can be programmed for specific functions and applications [2]. As a result, FPGAs are targeted for acceleration for various problems.

As coprocessors, FPGAs have shown remarkable speedups for certain applications. The main reasons for achieving these performance gains come from the deep pipelines and parallel execution units that FPGAs have to offer [3]. In addition, on-the-fly reconfiguration presents an oppurtunity to exploit multiple FPGA coprocessing designs allowing for a wider range of target applications. However, many of these applications will require external memory for the FPGA to access in order to solve larger problems. Therefore, a smart memory interface is crucial in order to achieve the potential performance benefits provided by FPGAs [14].

Generally, applications that require computational acceleration involve floating-point calculations. For this reason, the memory controller was designed specifically for reading and writing floating point values. An advantage of using floating-point representation is the wide range of values that can be represented [16]. Conversely, a number may not need as many bits to be represented accurately. For example,

assume a value can be represented accurately with 40 bits. On a normal processor, this number would require using double precision (64-bit) representation and a double precision floating-point unit. On the other hand, an FPGA can be programmed to handle 40-bit floating-point numbers that use smaller registers and smaller floating-point units. This results in extra space to allow for more concurrent units that will increase parallelism and thus performance. In order to accomodate this feature, the memory controller was designed to handle floating-point numbers with arbitrary precisions up to 64 bits.

The research presented within this thesis discusses the design and implementation of a memory controller for FPGA applications using floating-point numbers. The rest of the content will be laid out as follows. First, the platform that enabled such research is given. Second, the FPGA design will be presented with a particular emphasis on the design choices that were made to achieve a robust and efficient controller. Next, an overview of the software design will be given which will make the FPGA useful as a coprocessor. Finally, results will be shown to prove the memory controller's effectiveness for some given implementations.

Chapter 2

Hardware Design

This chapter will describe the hardware design, including the actual FPGA design and the development platform that makes all of this possible.

2.1 Platform

Before delving into the actual design, the platform that enables this idea of a coprocessor design needs to be introduced. This platform was GiDEL's PROCStar III. The PROCStar III system combines 4 ALTERA Stratix III 260E FPGAs onto a PCI Express board. Essentially, this board is connected through the PCI Express to a host processor to enable strong co-processing between a standard PC operating system and the FPGA acceleration. The FPGAs are Altera parts, so Quartus II software is used to compile HDL designs.

GiDEL's PROCDeveloper's Kit, in combination with the PROCStar III system, provides the user with a foundation to merge a unique FPGA design with a software application. The development kit provides a few key features resulting in an easier design process. The first feature is PROCWizard which is a software application that adds hardware and software connections to the FPGA design for the designer [11]. The application creates a top level HDL file to connect to the user design and ties hardware and software interfaces modules to the top level. It combines all of this

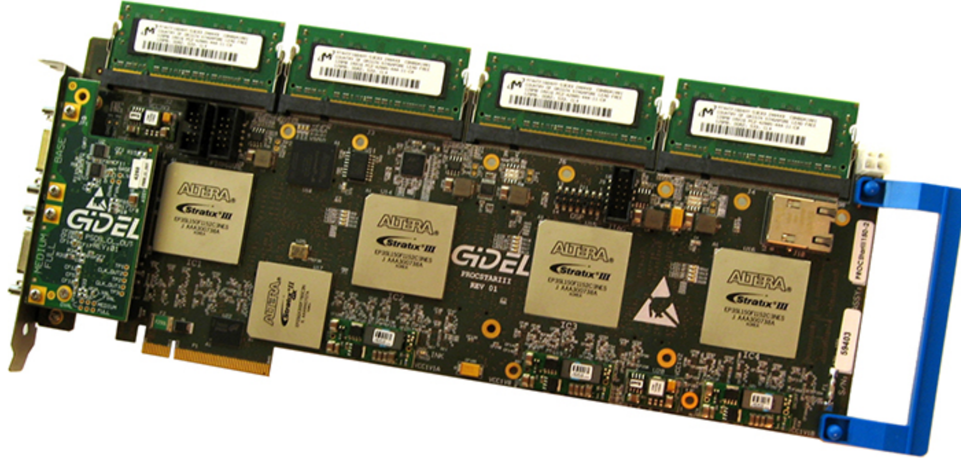

Figure 2.1: PROCStar III Board.

into a Quartus Project File to be compiled and generates a C++ Class Application Driver to interface these modules from software. The second feature provided by this development kit is the PROC Application Programming Interface (PROC API) which provides a set of functions used to access the PROC boards [10]. This API uses the application driver created by PROCWizard to communicate with the generated HDL design via the PCI express bus. The API is also used to perform hardware initializations, load FPGA designs, and set clock frequencies. The third feature that was used was the PROCMultiport IP [12]. This feature allows rapid parallel access to on-board SDRAM from the FPGA, as well as interfacing software to the SDRAM to allow large memory transfers over the PCIe bus.

In essence, the features above give the PROCStar III system the abstraction of being a coprocessor. The PROCStar III platform provides quick development, on-the-fly reconfiguration, hardware and software co-design, and high performance IPs.

2.2 FPGA Design

This section will describe the entire FPGA design in a top-down approach. The modules that will be described were written in VHDL and compiled using Quartus II software.

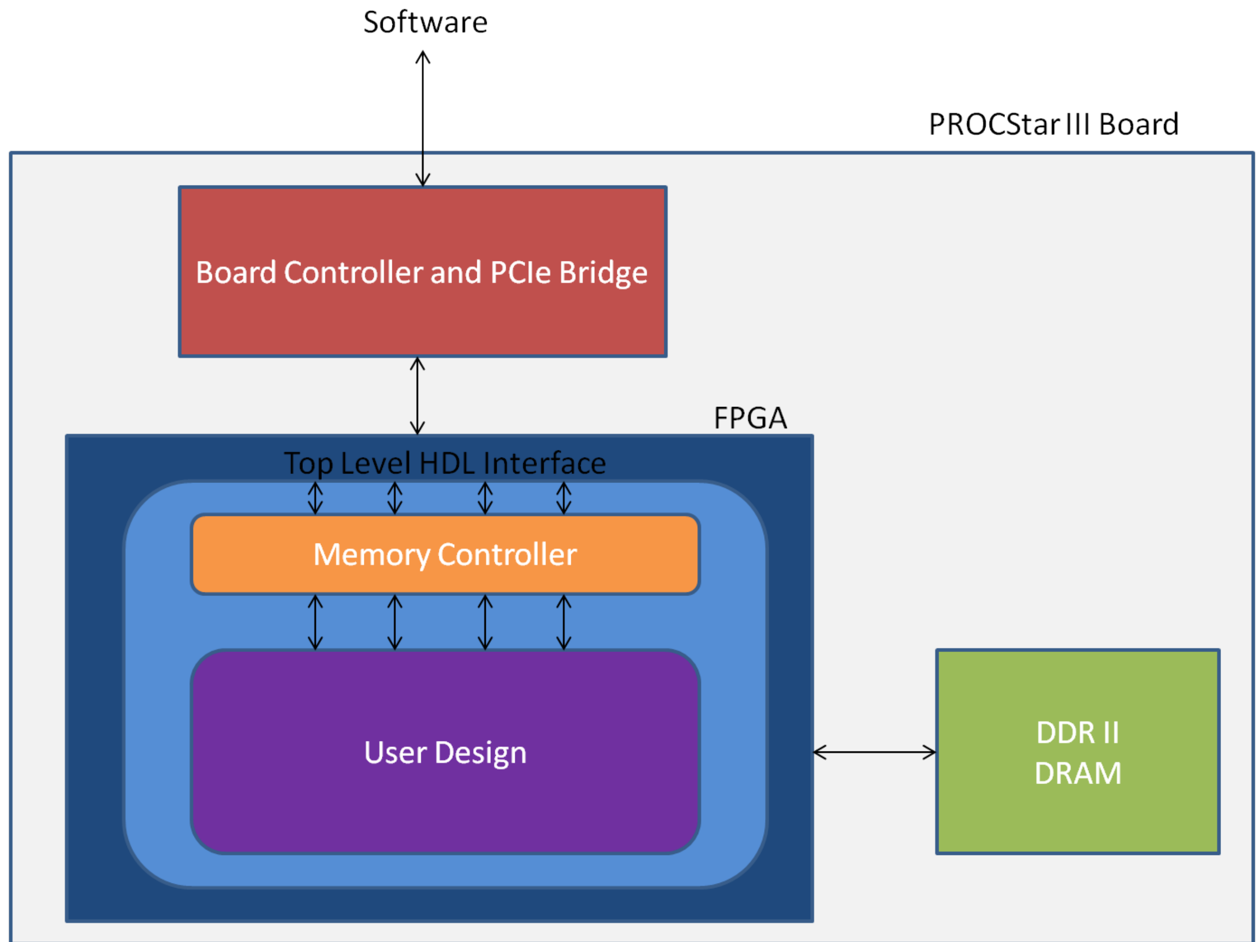

Figure 2.2: System Design Overview.

2.2.1 Top Level Module

The top level module (as shown in Figure 2.2) is the part of the design that controls all of the interfaces to outside peripherals, including the software and DRAM. This module was initially generated using PROCWizard. PROCWizard is a tool that helps users automatically connect software and memory to the HDL application.

For this design, PROCWizard was used to connect signals resident on both the FPGA and software in order to control the FPGA application. In particular, the software used signal 'Start' to control when computation on the FPGA should begin, and the FPGA used signal 'Done' to signal to software when the FPGA had finished its computation. In addition, PROCWizard was used to connect the PROCMultiport

IP to the top level design. The PROCMultiport IP is an HDL design IP that connects the FPGA to the SDRAM, as well as connecting the software through the FPGA to the SDRAM. This IP allows for quick memory transfers from the host processor to the SDRAM that will be accessible by the FPGA.

At this point, PROCWizard has created a module that will allow the software to control the FPGA and send data to memory that can be accessed by the FPGA application. These are the two essential functions that must be provided in order to have a coprocessing enviroment. The signals that coordinate directly with software are just that - signals. Therefore, these signals are easily tied into the user design. On the contrary, correctly connecting into the FPGA memory, or the SDRAM, is difficult to implement. The need for a memory controller is apparent.

The design of an intuitive and flexible memory controller will be discussed in the next section, but one more addition to the top-level design is needed. As of right now, the PROCMultiport IP provides the interface to the SDRAM, but is only routed to the software. This IP also needs to have the option of being routed to hardware or the SDRAM is useless to the FPGA application. So, a hardware/software control signal was created to toggle the PROCMultiport IP between the HDL design and the software design as show in Figure 2.3.

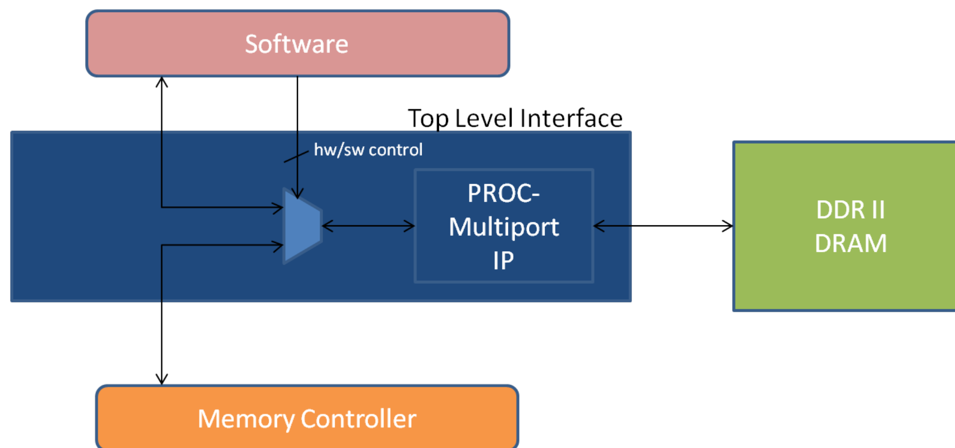

Figure 2.3: Toggle signal that gives memory control to Hardware or Software.

2.2.2 Memory Controller

As stated above, GiDEL's PROCMultiport IP is used as the top level interface to memory. The PROCMultiport IP is a memory controller by itself, but it does not provide certain features that are required to make the it useful for actual design. As a result, an extension to this IP was designed to provide some key benefits. Four main features went into the design of the memory controller: usability, flexibility, scalability, and performance. The following sections will present the design of the memory controller with respect to these features.

Usability

The first feature that was implemented into the design was simplifying the memory controller's usability so that a user could focus more on their own design. The PROCMultiport IP required very precise timing and signaling that was unintuitive and difficult for user implementation. The timing diagram in Figure 2.4 and the description below shows the compexities required to read and write to memory [12].

The steps required to read from memory using the PROCMultiport IP requires specific signaling. First, you have to load **addr_rd** with starting address. Then, assert **start_rd** signal high for 3 clocks to reset the port and **start_rd** signal low to allow FIFO to read from the port. Wait for FIFO to become non-empty by polling **almost_empty_rd** signal, delay 1 clock, and assert **select_rd** signal high to start reading from FIFO. Finally, read values sequentially from memory at each clock and assert **select_rd** signal low when all values read.

The steps required to write to memory using the PROCMultiport IP are similar. First, load **addr_wr** with starting address. Next, assert **flush_wr** signal high to flush the FIFO for writing and **start_wr** signal high for 3 clocks to reset the port. Then, assert **start_wr** signal low. Wait for **almost_full_wr** to assert low, delay 1 clock, and assert **select_wr** signal high to start writing from FIFO. Finally, present values

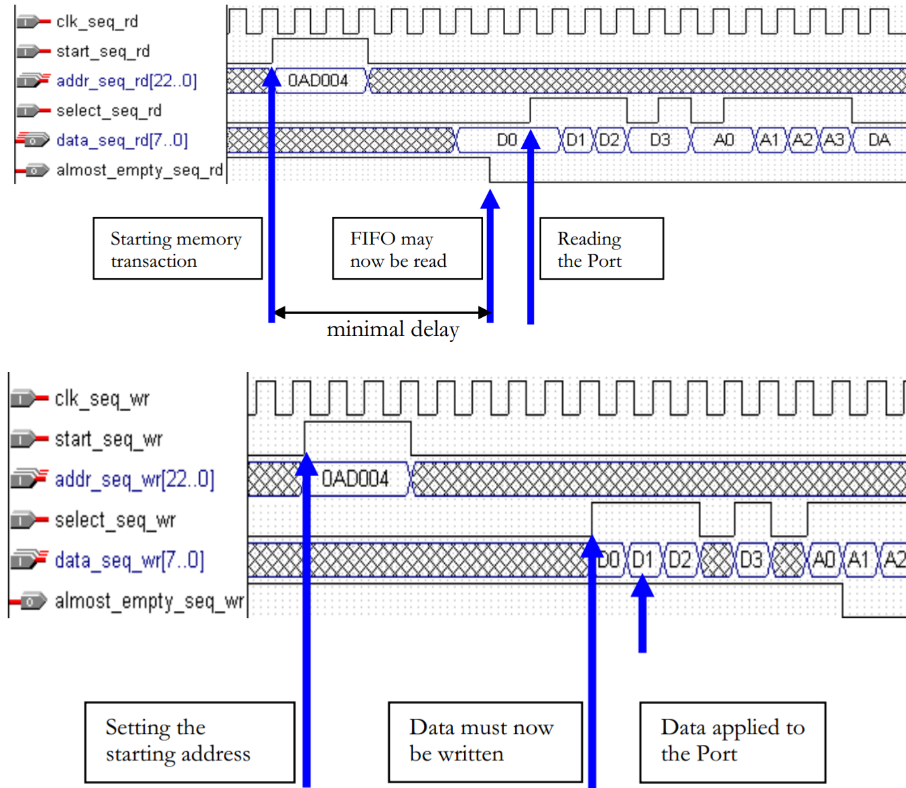

Figure 2.4: Timing Diagram for PROCMultiport IP for Reading and Writing to Memory [12].

to write to memory at each clock and assert **select_wr** signal low when all values written.

Clearly, reading and writing to memory using PROCMultiport IP can quickly get frustrating using all of these signals. This does not even mention the precise timing constraints required to poll these signals and present data at the appropriate times. Luckily, the memory controller that was designed will take care of all of this for you and provide a much simpler interface.

The steps required to read and write memory using the Memory Controller begins with asserting **read** or **write** high with **addr** set to the desired address. Then, wait for **data_ready** or **write_done** to assert high. Finally, assert **read** or **write** low.

The usability of the above Memory Controller is far superior to the original. The control is implemented by the controller itself and is not left up to the user. This saves a lot of hassle and results in much quicker design times.

Flexibility

Perhaps the most useful attribute of the Memory Controller is its flexibility. It supports configurable precision for floating point numbers. Allowing variable precision gives the designer the oppurtunity to trade some accuracy for performance. For this particular platform, the software interface enables designs with different precisions to be loaded onto the FPGA on the fly. Designs can be coupled effectively to result in both better performance and sufficient accuracy.

As stated earlier, the Memory Controller supports configurable precision, meaning that the design has to be recompiled for different precisions. In order to change the precision of the Memory Controller, only a few top level constants need to be changed: PRECISION, MANTISSA, and EXPONENT. These are defined as constants inside of a package list associated with the design.

Keeping the software design simple was a crucial aspect of the Memory Controller design. As a result, the SDRAM was implemented to contain double precision values, so that the software could make simple memory transfers. The Memory Controller is what converts these double precision values down to the precision specified by the user. The controller also converts the user precision back to double precision before storing the values. This is shown in Figure 2.5.

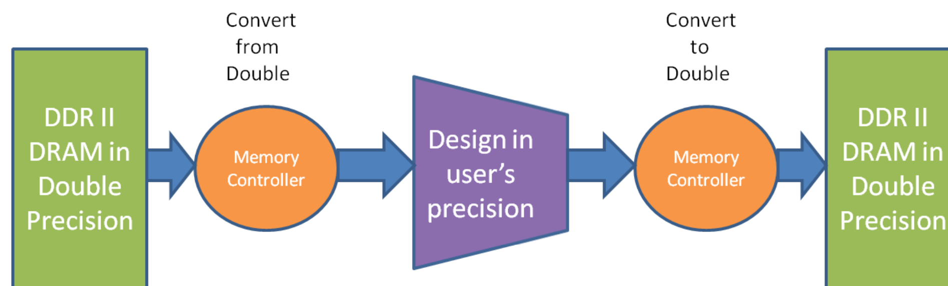

Figure 2.5: Conversion Process to and from SDRAM.

Floating point numbers are represented using three fields: sign, exponent, and mantissa. The representation for an arbitrary floating point number with given mantissa and exponent is shown below.

$$width_of_mantissa = m \tag{2.1}$$

$$width_of_exponent = e \tag{2.2}$$

$$total_width = precision = m + e + 1 \tag{2.3}$$

sign	exponent	mantissa
bit[m+e]	bits[m+e-1...m]	bits[m-1...0]

$$fp_representation = 1.xxxx * 2^{yyyy} \tag{2.4}$$

where

$$xxxx = mantissa \tag{2.5}$$

$$yyyy = exponent - bias \tag{2.6}$$

$$bias = 2^{n-1} - 1 \tag{2.7}$$

where n is number of bits in exponent field.

For conversion, only the exponent and mantissa fields need to be converted. Double precision is 64 bits wide: 1 sign bit, 11 exponent bits, and 52 mantissa bits. The method for converting from double precision to a precision with arbitrary mantissa (m) and exponent (e) widths is explained below.

$$bit[m + e] = bit[63] \tag{2.8}$$

$$bit[m + e - 1] = bit[62] \tag{2.9}$$

$$bits[m+e-2...m] = bits[50+e...52] \tag{2.10}$$

$$bits[m-1...0] = bits[51...52-m] \tag{2.11}$$

This next example shows a double precision value of 1,317,545 converted to a 24 bit precision with exponent width of 6 and mantissa width of 17. In this case, the result is 1,317,544, which is slightly less precise than the original.

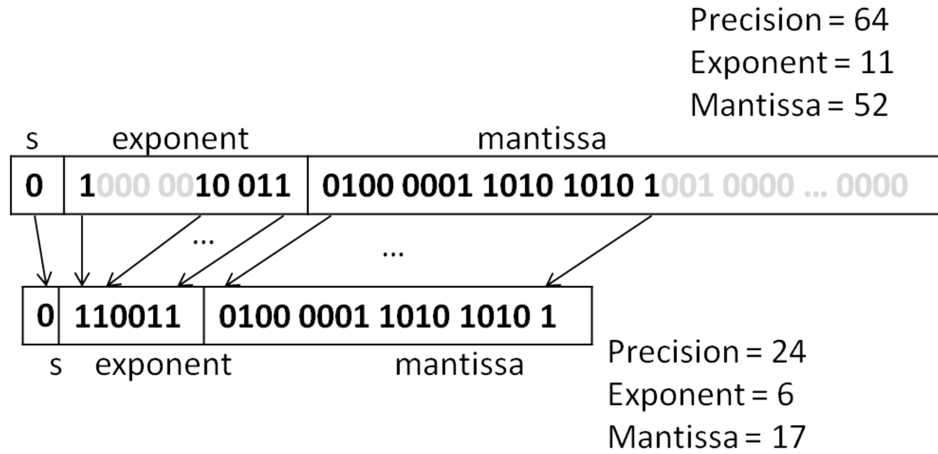

Figure 2.6: Conversion from Double Precision to 24 bit precision with exponent width 6 and mantissa width 17.

Converting back to double precision from an arbitrary precision is not quite as straight forward. The leading exponent bit plays a key factor in determining how to convert the exponent back to the double precision value. However, it is still quite simple. If the leading exponent bit is a '1', the bits that are inserted into the exponent are '0's. If the leading exponent bit is a '0', the bits that are inserted are '1's. Using the same methodology as before, this process is described below:

$$bit[63] = bit[m+e] \tag{2.12}$$

$$bit[62] = bit[m+e-1] \tag{2.13}$$

$$bits[61...51+e] = NOT(bit[m+e-1]) \tag{2.14}$$

$$bits[50 + e...52] = bits[m + e - 2...m] \tag{2.15}$$

$$bits[51...52 - m] = bits[m - 1...0] \tag{2.16}$$

$$bits[51 - m...0] =' 0' \tag{2.17}$$

Figure 2.7 shows the conversion when the leading exponent bit is a '1'.

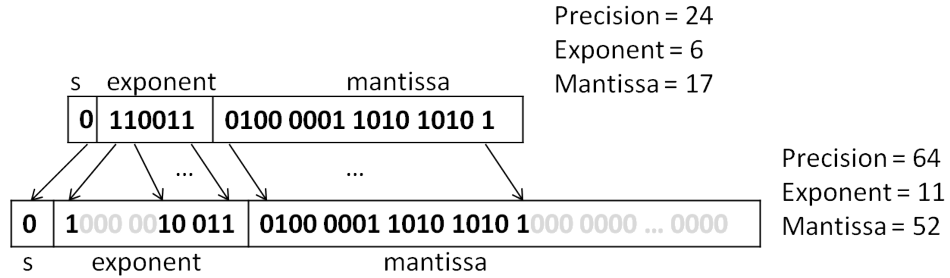

Figure 2.7: Conversion from 24 bit precision with exponent width 6 and mantissa width 17 to Double Precision.

Figure 2.8 shows the conversion when the leading exponent bit is a '0'.

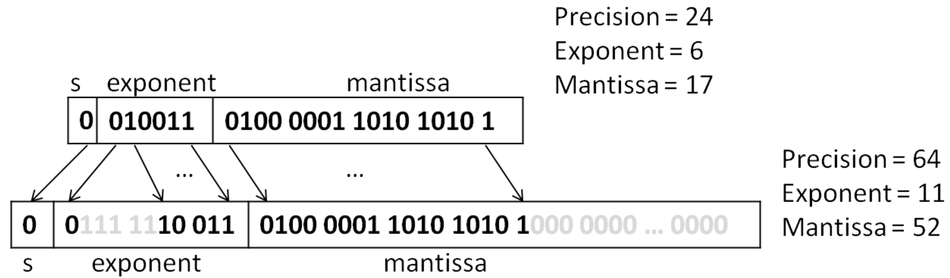

Figure 2.8: Conversion from 24 bit precision with exponent width 6 and mantissa width 17 to Double Precision.

The simple proof to show that the exponent conversion is correct is to show the values of the exponent (2.6) in the floating point representation equation (2.4):

$$fp_representation = 1.xxxx * 2^{yyyy}$$

$$yyyy = exponent - bias$$

Case 1 based on figure 2.7:

24-bit precision

$$bias = 2^{n-1} - 1 = 2^{6-1} - 1 = 31$$

$$exponent = 51$$

$$yyyy = exponent - bias = 51 - 31 = 20$$

Double precision

$$bias = 2^{n-1} - 1 = 2^{11-1} - 1 = 1023$$

$$exponent = 1043$$

$$yyyy = exponent - bias = 1043 - 1023 = 20$$

Case 2 based on figure 2.8:

24-bit precision

$$bias = 2^{n-1} - 1 = 2^{6-1} - 1 = 31$$

$$exponent = 19$$

$$yyyy = exponent - bias = 19 - 31 = -12$$

Double precision

$$bias = 2^{n-1} - 1 = 2^{11-1} - 1 = 1023$$

$$exponent = 1011$$

$$yyyy = exponent - bias = 1011 - 1023 = -12$$

Note: It is left up to the user to determine if the precision, mantissa, and exponent are wide enough to satisfy a desired accuracy!

Performance

The most important aspect taken into account when designing the Memory Controller was performance. If the Memory Controller is poorly designed, the overall acceleration of the application will be limited. Two key aspects attributed to achieving better performance: larger memory transfers and data reuse.

The reason that large memory transfers are needed is because there is a required setup time to access the SDRAM. The PROCMultiport IP uses FIFO buffers to shuttle data to and from memory to make connection and timing easier. When using these FIFOs, enough data must fill up the FIFO before it can begin transferring data to and from memory. As a result, every memory transaction incurs this delay penalty to partially fill up the FIFO. Using larger memory transfers instead of smaller transfers helps negate this delay factor. An example details this below.

The board used was a ProcStar III Board which defines the FIFO Depth as 256 words, so the delay required to fill up the FIFO before a memory transfer is:

$$delay = 16 + (FIFO\ depth * 1/8)\ clocks \tag{2.18}$$

$$delay = 16 + (256 * 1/8)\ clocks \tag{2.19}$$

$$delay = 48\ clocks \tag{2.20}$$

To show the difference between larger and smaller memory transfers, the read of a 128x128 matrix for different size transfers is explored. Assume a small transfer is 32 words and a large transfer is 1024 words. After the initial delay, one word per clock is presented at the end of the FIFO.

Small Transfer (32 word blocks)

$$\#\ of\ reads = 128 * 128 = 16384$$

$$\#\ of\ transfers = \#\ of\ reads/32 = 512$$

$$total\ delay\ penalty = \#\ of\ transfers * delay = 512 * 48 = 24576\ clocks$$

$$total\ read\ time = total\ delay\ penalty + \#\ of\ reads = 24576 + 16384 = 40960\ clocks$$

Large Transfer (1024 word blocks)

$$\#\ of\ reads = 128 * 128 = 16384$$

$$\#\ of\ transfers = \#\ of\ reads/1024 = 16$$

$$total\ delay\ penalty = \#\ of\ transfers * delay = 16 * 48 = 768\ clocks$$

$$total\ read\ time = total\ delay\ penalty + \#\ of\ reads = 768 + 16384 = 17152\ clocks$$

As shown above, the bottleneck for small memory transfers quickly becomes the delay penalty. For larger transfers, the delay penalty is almost completely negated.

$$speedup = 40960/17152 = 2.39$$

In order to take advantage of this aspect for different designs, the size of the memory transfer is configurable. A memory transfer can be viewed as reading in a very large cache line. The top level package list has a configurable parameter LINE_SIZE which dictates the size of the memory transfer. Based on the size and requirements of the design, this parameter can be as large as it needs to be to achieve better performance.

The second method for achieving better performance from the memory controller is memory caching for data reuse. For applications that require data reuse, caching can significantly increase performance. FPGAs also have the benefit that the cache can be manually controlled for optimal usage. The performance improvement provided by caching will vary based on the application, but caching will always be useful. The user design section and results will cover the benefits provided by caching. This section merely shows how it works.

The cache is set up based on the memory transfer size (or LINE_SIZE) that was discussed earlier. Without caching, every memory reference will read the data from SDRAM resulting in a 48 clock delay time and 1 clock per word that is read. With caching, this same penalty occurs for the first time a line of data is read. However, when this line is read, the address (or tag) is stored. When a consecutive memory reference to the same location is made, a cache hit is generated and the data is immediately ready for use avoiding the cost to read it from the SDRAM again. The parameter LINE_SIZE determines how big the cache line is and the size of the tag. Therefore, each memory reference checks the tag associated with it and determines whether there is a hit or a miss. Cache misses read in LINE_SIZE words from the SDRAM and stores the upper part of the address in the tag field. The cache initially starts out invalid to avoid the situation where the tag is equal to the address being read at the start.

2.2.3 User Design

The user design is the main piece of the design that dictates how the memory controller should be customized and used. Based on the application, certain design choices can be made to improve performance. The user design that was used in this research was matrix multiplication. This design was used in order to show both the memory controller's correctness and effectiveness. First, the overview of the design will be given. Second, the design will be used to introduce how to interface the memory controller in general. Finally, the customizations to the memory controller based on the design will be shown.

Recall that matrix multiplication is:

$$C = A * B \tag{2.21}$$

The data used for the matrix multiplication is controlled by software, so it can easily be manipulated and transferred intelligently to the FPGA by the software

beforehand. For this reason, matrix B is sent in as a transposed version in order to make memory transfers intuitive and fast for the application. The matrix multiplication can now be viewed as:

$$C = A * B^T \tag{2.22}$$

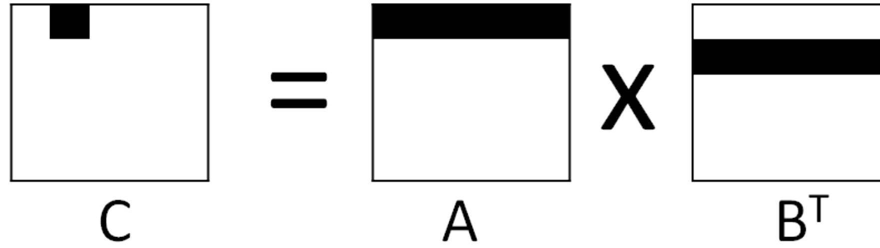

Figure 2.9: Iteration of matrix multiply.

Keep in mind, the goal of this research was not to optimize the performance for this particular implementation of matrix multiplication. The matrix multiplication is merely used as an example to show the benefits and correctness of the memory controller. The next section will describe how the matrix multiplication was implemented.

The matrix multiplication was performed one row in A and one column (or transposed row) in B at a time. Both a row of A and a column of B are read in from memory. The entire row and column are fed into a chain of floating point multipliers. The output of these multipliers are connected to another chain of floating point adders that will reduce the result down to a single value to store in matrix C. This process can be seen in Figure 2.10.

The floating point units that were used in the design were Altera's Floating Point Megafunctions. These Megafunctions only provided 32-bit and 64-bit support, but that was sufficient enough to prove the concepts of configurable precision for the memory controller. The specs of the floating point multiplier and adder for both precisions are summarized in Table 2.1.

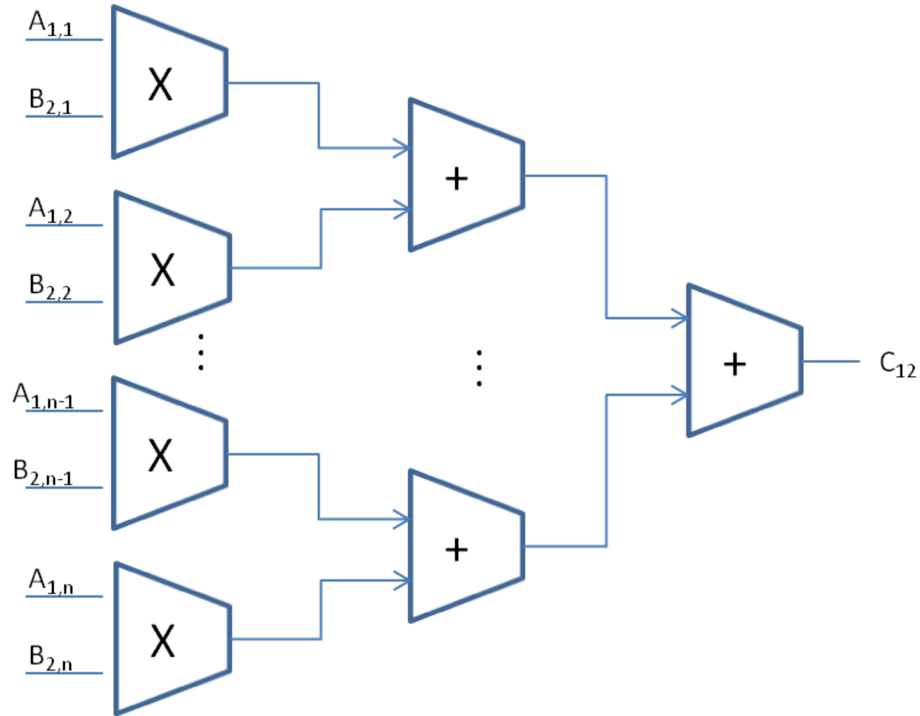

Figure 2.10: Hardware view of one iteration of matrix multiply.

The reduction stage of the matrix multiplication is not exactly what is shown in Figure 2.10. The adders in the second stage are actually reused by feeding the outputs of two adders into the inputs of a single adder based on what step of the reduction phase we are on. For an NxN matrix, this design improvement saves N/2 - 1 adders. Therefore, a total of N multipliers and N/2 adders are used to compute a single element of C at a time.

For every element in C a different row and column combination of A and B are multiplied which requires a new memory reference each time. This is where the need for a smart memory controller comes into play. If not done optimally, the memory interface can quickly become the bottleneck for this matrix multiplication.

The matrix multiplication control unit is the part of the user design that interfaces to the memory controller using a series of addressing and handshaking signals. For this design, three addresses are used: **addr_A**, **addr_B**, and **addr_C**. These are the three output addresses that correspond to where A, B, and C are located in SDRAM

	32-bit		64-bit	
Megafunction	Latency (in clocks)	Resource Usage	Latency (in clocks)	Resource Usage
Adder	7	169 LUT 368 reg	7	301 LUT 676 reg
Multiplier	11	4 dsp_18bit 55 LUT 389 reg	11	9 dsp_18bit 205 LUT 718 reg

Table 2.1: Specs for Altera's Floating Point Megafunctions.

or in cache. Three output signals **read_A**, **read_B**, and **write_C** tell the memory controller when the address is set and the user is ready to read or write data to or from memory. Input signals **data_ready** and **write_done** signal to the user when the data has been read in from or written to SDRAM respectively. The control unit makes reading and writing data relatively simple. A request is sent out to read or write memory at a certain location and a signal is sent back when this request has finished.

A few customizations were made to the memory controller to make it more suitable for the matrix multiplication application. The LINE_SIZE parameter was chosen to be the size of a dimension of the matrix. This is necessary because the matrix multiplication processes one row and column at a time, so it needs the LINE_SIZE big enough to hold a row or column of the matrix. Three separate caches were used and maintained, one for each A, B, and C. The caches for A and B are maintained as read/write caches. The cache for C is maintained as a write only cache.

All of the caches were initially made the same size using LINE_SIZE as the size of the cache. LINE_SIZE was chosen based on the maximum amount of floating point units that would fit into the FPGA which also dictates the size of the matrices to be processed. After doing an initial fit of the maximum matrix that can be processed based on the precision and the three caches that are used, the FPGA had some leftover

space. Rather than wasting the space, the space was used to increase the cache size of matrix B. The reason matrix B's cache was chosen to be enlarged was because matrix B is strided through more frequently than A or C. The nature of matrix multiply already creates a solid foundation of cache hits for both A and C. Therefore, the cache for matrix B is targeted to achieve a better performance improvement. The size of the cache for B should be the largest multiple of 2 that will fit into the design. This parameter is called CACHE_SIZE in the top level package list.

Chapter 3

Software Design

The ability of FPGAs to be coprocessors relies heavily on the software design. For large problem sizes, many FPGAs will need to be used and scaled together. The management and coordination of these FPGAs must be maintained through software. The following chapter will describe the development of the software design and how it interfaces with the FPGA to achieve an efficient and scalable design.

3.1 Software and FPGA Interface

As stated in previous sections, GiDEL's PROCDeveloper's Kit provides the software tools PROCWizard and PROC API. The PROCWizard tool creates the C++ class application driver. PROC API provides a set of functions to access the PROC board and to use the objects created by the application driver.

The C++ class application driver is essentially a header file that provides an object for every variable on the FPGA that needs to have an interface to software. The driver allocates a location in memory that is tied to the FPGA design through the PCIe to communicate through variables. When an object is changed in software, this change also takes place on the FPGA.

The objects that were used as directly shared variables were **START**, **DONE**, and **HW_SW_CONTROL**. The other objects were referenced using the PROC API for

simplicity and will be described later. The object, **START**, was used as input to the FPGA to signal when to begin processing. **DONE** was connected as output from the FPGA to signal to the software when it was done processing. **HW_SW_CONTROL** was used as input to the FPGA to give control to either the FPGA or software for memory transactions. Clearly, each of these signals are easy to manipulate and only require a 1 or 0 to coordinate the software with the FPGA.

The more difficult part is preparing the FPGA so that it is equipped with everything that it needs to begin processing. This is where the PROC API is used. Many other objects were created by PROCWizard for the application driver. These objects are meant to be used by the functions provided by the API and not directly manipulated like the signals above. The functions used for the design are described in Table 3.1.

Function	Description
LoadIC	Loads and configures a FPGA design (.rbf file) from a specified file path onto a particular FPGA
SetClock	Sets the clock values for the FPGA
CreateDMABuffer	Creates a buffer, locks the memory and performs all the necessary initializations for the DMA engine
GetUserBuffer	Gets the pointer to the data buffer from the buffer handle created by CreateDMABuffer
RunDMA	Runs a DMA transfer to/from a buffer prepared using the CreateDMABuffer() method. Non-blocking
WaitDMADone	Suspends the program execution until the DMA transfer on the specified channel is finished
RemoveDMABuffer	Removes the buffer

Table 3.1: Functions from PROC API used in design.

The functions above are very helpful. The LoadIC function allows for designs to be loaded onto an FPGA on the fly on a specific FPGA. The DMA functions enable the software to quickly and easily send large chunks of data to the FPGA or read large chunks out. With the interface mechanism described above, the FPGA now has the capability to function as a coprocessor.

3.2 Program Overview

This section will describe the software program that was written to control the matrix multiplication performed by the FPGAs. The program is built around the application driver described above. Essentially, the program will configure and initialize the FPGA, perform the matrix multiplication, obtain the results, and compare the results to a known solution.

The FPGA can only handle a maximum size matrix. However, from the software side, a blocked version of matrix multiply can be implemented to multiply any size matrices by using the FPGA multiple times. The following is a summary of the steps required to carry out a matrix multiplication on one FPGA from the software side. A more detailed implementation is described later which includes using multiple FPGAs and certain design choices to enhance performance.

1. Initialize C++ class driver which loads the FPGA with the design using LoadIC and ties it to software.

2. Allocate and initialize matrices A, B, and C on the host processor with random values.

3. Create read and write buffers between host and PROC board using CreateDMABuffer.

4. Fill write buffer with blocks of matrices A, B, and C (a block being the size of matrix that the FPGA is configured to multiply).

5. Send buffer to PROC board DRAM using RunDMA on the write buffer.

6. Wait for transfer to complete using WaitDMADone.

7. Signal memory control to the FPGA by changing the signal **HW_SW_CONTROL** to a 1.

8. Signal the FPGA to begin matrix multiply by changing **START** to a 1.

9. Wait for FPGA to change signal **DONE** to a 1.

10. Signal memory control to the host by changing the signal **HW_SW_CONTROL** back to a 0.

11. Read buffer from PROC board DRAM using RunDMA on the read buffer.

12. Wait for transfer to complete using WaitDMADone.

13. Accumulate new C matrix with current C matrix on host.

14. Reset **START** signal to 0 which resets **DONE** signal on the FPGA so another iteration can be performed.

15. Repeat steps 4-14 as needed until the entire matrix has been iterated through and multiplied.

16. Check resulting matrix C against a software computed known solution.

17. Free buffers and memory.

The program described above allows the execution of any size of matrix multiplication. It can be easily manipulated to work for functions other than matrix multiplication. The foundation of the program is to be able to configure the FPGA, perform the desired function by communicating with the FPGA, transfer data back and forth, and observe the results.

Chapter 4

Implementation and Results

The following chapter will present the implementations used to test and validate the memory controller. In particular, certain design choices will be compared against each other and the results will be shown. The implementation is based on the user design which is matrix multiplication. Design choices will vary based on the user design, but the implementations used for matrix multiplication should be easy to modfiy or extend for different designs.

4.1 Hardware Implementation and Performance Models

The hardware design choices that were made for the memory controller were based on two key factors: precision and area. These two factors happen to directly affect each other. As stated in Chapter 2 in the User Design section, N floating-point multipliers and N/2 floating-point adders are used for the design. The goal is to choose the highest value of N that is a power of 2 that will fit into the design. The FPGA area factor comes into play determining this N value. However, the precision of the floating-point units determines the size of the units, so the precision also comes into play. Consequently, the overall goal is now to minimize the precision to a desired

accuracy and maximize the N parameter. Once these values have been optimized, the remaining space should be used to maximize the cache size. As a result, the FPGA should be almost fully utilized and perform better.

Altera provides megafunctions for single (32-bit) and double (64-bit) precision, but they do not provide configurable precision floating-point units for arbitrary precisions. Therefore, the two implementations that were used for testing were single and double precision. Even so, single and double precision floating-point units provide an excellent comparison to the effects precision has on area and accuracy. The number of floating-point units for each precision is presented in Table 4.1.

Precision	N	# of floating point multipliers	# of floating point adders
Single (32-bit)	128	128	64
Double (64-bit)	64	64	32

Table 4.1: Number of floating-point units in design that can fit into the FPGA with given precision.

As shown in Table 4.1, precision has a huge impact on the hardware area required for a floating-point unit. For this design, the number of floating-point units dictates the size of matrix multiplication that can be performed at a time. At the same time, the memory cache footprint remains the same because two 32-bit values can fit in the same space that one 64-bit value can. As stated before, the remaining space is used to enlarge the cache that holds the B matrix. For this implementation, the cache size for matrix B is enlarged from 1 cache line to 16 cache lines. The fitter summary provided by the Quartus II software is provided for both precisions in Table 4.2.

Because of the fact that the application is being run on a designed and programmed FPGA, the hardware time required to complete a block of matrix

	precision : 64, exp : 11, mant : 52 N : 64, cache line size : log2(N) = 6 # cache lines: A = 1, C = 1, B = 16	precision : 32, exp : 8, mant : 23 N : 128, cache line size : log2(N) = 7 # cache lines: A = 1, C = 1, B = 16
Family	Stratix III	Stratix III
Device	EP3SE260F1152C4	EP3SE260F1152C4
Logic Utilization	100%	98%
Combinational ALUTs	161,849 / 203,520 (80 %)	160,736 / 203,520 (79 %)
Memory ALUTs	320 / 101,760 (< 1 %)	320 / 101,760 (< 1 %)
Dedicated logic registers	149,808 / 203,520 (74 %)	158,471 / 203,520 (78 %)
Total registers	150294	159214
Total pins	736 / 744 (99 %)	736 / 744 (99 %)
Total virtual pins	0	0
Total block memory bits	376,848 / 15,040,512 (3 %)	376,848 / 15,040,512 (3 %)
DSP block 18-bit elements	640 / 768 (83%)	512 / 768 (67 %)
Total PLLs	2 / 8 (25 %)	2 / 8 (25 %)
Total DLLs	1 / 4 (25 %)	1 / 4 (25 %)

Table 4.2: Fitter Summary provided by Quartus II Software.

multiply can be directly calculated in clock cycles. The runtime consists of two primary components: calculation time and memory time. Calculation time is less variable and much easier to compute, so it will be looked at first. However, the purpose of this research is tied to the memory portion, so many improvements can be made to the calculation time. The calculation time is merely discussed for reference and to be thorough.

The multiplication time is technically broken up into subsections as shown in Figure 4.1. The overall matrix is divided into smaller blocks that are multiplied together. Inside of these blocks, each row is multiplied by each column as a vector multiply. Distinguishing these parts makes describing the model for runtime easier to understand.

The following variables will be used in the runtime models:

$$N = square\ matrix\ size$$

$$blocksize = size\ of\ block\ from\ original\ matrix$$

$$time_{add} = number\ of\ clocks\ to\ complete\ a\ floating\ point\ add$$

$$time_{multiply} = number\ of\ clocks\ to\ complete\ a\ floating\ point\ multiply$$

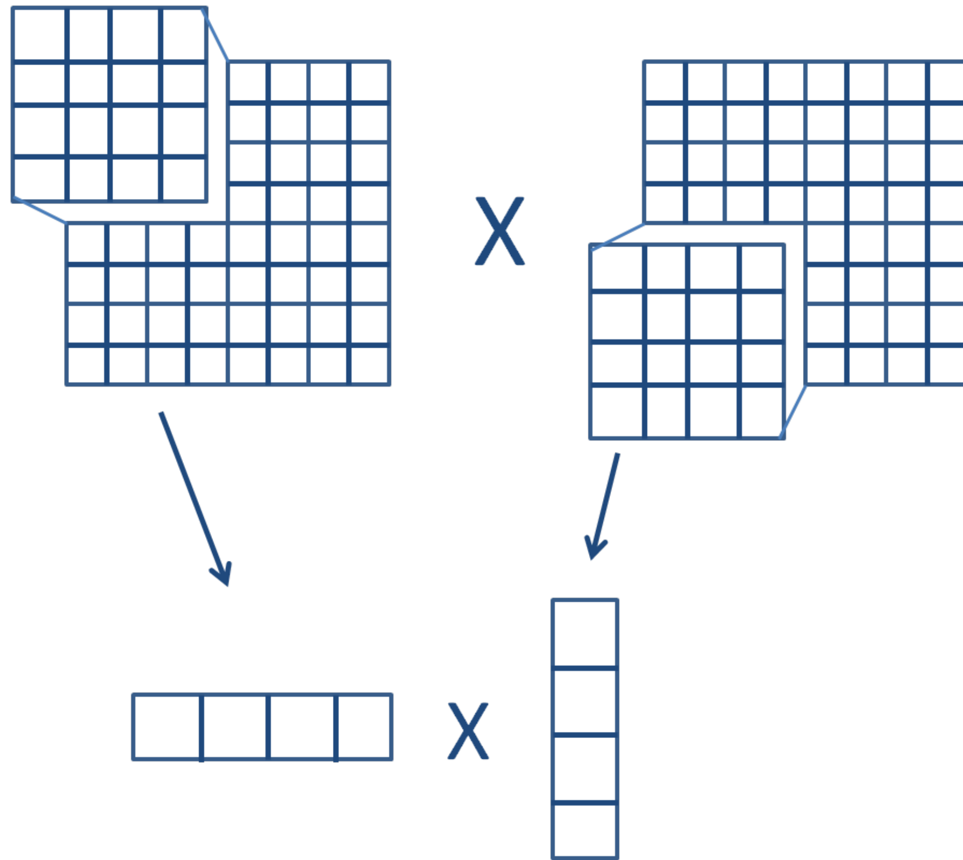

Figure 4.1: Matrix multiply divided into blocked matrix multiply and then vector multiply.

Starting with vector-vector multiply, the number of clocks to complete a single vector-vector multiply of size blocksize is:

$$time_{vector} = time_{multiply} + log_2(blocksize) * time_{add} \tag{4.1}$$

The equation above represents what is happening in Figure 2.10. There is one level of floating point multiply and then a chain of floating point adders to arrive at a single value. This process is repeated for every row and column in each block. The time needed to multiply an entire block without taking into account memory time is described below.

$$time_{block} = blocksize^2 * time_{vector} \tag{4.2}$$

The memory time required to perform this blocked matrix multiply is a bit more complicated. There are two memory transfers to consider: the time to transfer data across the PCIe bus to and from the PROCBoard and the time spent reading and writing memory using the FPGA. Transferring data across the PCIe bus is difficult to model because it depends on the system that the platform is running on, so this memory time will be referred to as *overhead*. The FPGA memory transfers can be modeled in three parts for this application: reading the A matrix, reading the B matrix, and writing the C matrix. The number of clocks used by the FPGA for memory operations for one block of the matrix multiply defined below.

$$time_{readA} = (FIFO\ init\ time + blocksize/2) * blocksize \tag{4.3}$$

Inside of the parentheses is the amount of clocks required to read an entire row of A. The *FIFO init time* is the setup time required to initialize the FIFO and read from SDRAM. This time is required for every set of memory reads and writes. The memory controller reads and writes two values to SDRAM per clock, so the *blocksize* term inside of the parentheses is divided by 2. The other *blocksize* term is the number of rows in A that need to be read. Each row of A is reused *blocksize* times before having to move to the next row, so the memory does not need to be referenced as frequently as the B matrix.

$$time_{readB_nocache} = (FIFO\ init\ time + blocksize/2) * blocksize^2 \tag{4.4}$$

Reading the B matrix from memory occurs more frequently. For each row of A, every column of B has to be referenced, hence the extra *blocksize* term. When there is enough room for caching part of the B matrix, part of the B matrix only needs to be read once. Therefore, the time reduces to:

$$time_{readB_cache} = (FIFO\ init\ time + blocksize/2) * (blocksize - cachesize) * blocksize$$

$$+ (FIFO\ init\ time + cachesize * blocksize/2) \tag{4.5}$$

If the application operates on a smaller matrix and has enough hardware to cache the entire matrix, the time becomes:

$$time_{read_fullcache} = FIFO\ init\ time + (blocksize/2) * blocksize \tag{4.6}$$

The resulting matrix has the same timing model as reading the A matrix, but for a different reason. A row of the C matrix is computed one element at a time. When a full row is computed, the entire row is written back to SDRAM. Therefore, the equation remains:

$$time_{writeC} = (FIFO\ init\ time + blocksize/2) * blocksize \tag{4.7}$$

Combining all of the factors from above, the required memory time to perform a single block of a blocked matrix multiply is

$$time_{memory} = time_{readA} + time_{readB} + time_{writeC} + overhead \tag{4.8}$$

where *overhead* is the memory time required to transfer memory from software as stated before.

4.2 Software Implementation

In order to make the hardware design useful, the FPGA must be controlled by software as described in Chapter 3. This section describes how the software should be implemented based on the platform used in order to achieve a more efficient and scalable design.

A given platform will have a certain number of FPGAs, X, connected to it through the PCIe bus. The goal is to achieve a parallelism of X based on the number of FPGAs. This would require completely overlapping the software portion with

the hardware portion. This is not possible, but can be approached using two key optimizations: overlapping software control and reduction with FPGA computation and threading FPGA control between processors.

Overlapping software with FPGA computation is quite simple. For a blocked matrix multiply, each FPGA is given blocks of the matrices to multiply. The results are read back and have to be reduced into a single matrix before moving on to the next iteration. In addition, the buffer to transfer the next iteration's data has to be filled with new blocks. This process and the reduction can be overlapped by performing them while the next iteration is run on the FPGA using a simple three step process: 1. Send data to the FPGAs and begin FPGA computation. 2. Fill buffer with next iteration's data and reduce last iteration's result. 3. Wait for FPGAs to finish computation and read data from FPGAs. As a result, step 2 is completely overlapped by the computation on the FPGAs.

Another way to increase the performance of the software design is to assign seperate threads to control different FPGAs. Doing this allows each thread to control its own data transfer between the CPU and FPGA and communicate with its FPGA. This eliminates a single thread having to sequentially transfer data and control communications between each FPGA which would slow down each iteration because of blocking calls. Ideally, there will be one processor per FPGA. If there is not, threading will still be benefitial because threads will context switch on longer blocking calls.

The software implementation can be optimized to partially overlap with the FPGA computation. Therefore, the software performance will be viewed as a constant term, $overhead_{software}$. $Overhead_{software}$ occurs for every iteration of the blocked matrix multiply, so it becomes a significant term. Another term that is needed, but mitigated when larger matrix computations are performed, is the initialization time required to load the FPGAs and initialize the matrices. This term is very small in comparison to the rest of the computation, especially on larger matrices, but will be included as $time_{initialize}$.

4.3 Overall Performance Model

The models for both the software and hardware can be combined to obtain the overall performance model for a single matrix multiplication on a single FPGA. The first term will be the initialization time required by software and only occurs once. The next term is a combination of the software and hardware terms for each iteration of blocked matrix multiply. These terms will have to be iterated through as outlined below:

$$time_{overall_per_block} = (time_{memory} + time_{block} + overhead_{software}) \tag{4.9}$$

$$time_{overall} = (time_{overall_per_block}) * (N/blocksize)^3 + time_{initialize} \tag{4.10}$$

The equation above is mostly predicated on the *blocksize* that is chosen. A smaller *blocksize* will result in a much larger term to be cubed. However, it can also result in a smaller $time_{overall_per_block}$. For larger matrices, though, the goal is to fit the maximum *blocksize* matrix multiplication in order to achieve the best performance.

When multiple FPGAs are used, the models change slightly. When there is at least one processor for each FPGA, the parallelism nearly equals the number of FPGAs and approaches the equation below:

$$time_{overall_parallel} = time_{overall}/(\#\ of\ FPGAs) \tag{4.11}$$

4.4 Expected Results

Numerous tests were performed to validate the memory controller for correctness and performance. Performance will be compared against various sizes of cache, single and double precision, different levels of software optimization, and the number of FPGAs.

For correctness, the matrix multiplication is performed and the resulting matrix is compared to a known result.

The environment that this was tested on is a GiDEL PROCStar III system that combines 4 ALTERA Stratix III 260E FPGAs onto a PCI Express board connected to an Intel Xeon CPU with 8 processors running at 2.27 GHz. Table 4.3 gives the parameters that were used for testing.

	Clock Rate (MHz)	adder time (clocks)	multiply time (clocks)	blocksize	FIFO Init Time (clocks)	cachesize
32-bit	87.5	7	11	128	48	0-16
64-bit	87.5	7	11	64	48	0-16

Table 4.3: Parameters used for different precisions.

The parameters shown in 4.3 lead to the following expected runtimes:

For single precision (32-bit):

$$time_{vector} = time_{multiply} + log_2(blocksize) * time_{add}$$

$$= 11 + log_2(128) * 7 = 60\ clocks$$

$$time_{block} = blocksize^2 * time_{vector} = 128^2 * 60 = 983,040\ clocks$$

$$time_{readA} = (FIFO\ init\ time + blocksize/2) * blocksize = (48 + 128/2) * 128 = 14,336\ clocks$$

$$time_{readB_nocache} = (FIFO\ init\ time + blocksize/2) * blocksize^2$$

$$= (48 + 128/2) * 128^2 = 1,835,008\ clocks$$

$$time_{readB_cache} = (FIFO\ init\ time + blocksize/2) * (blocksize - cachesize) * blocksize$$

$$+(FIFO\ init\ time + cachesize * blocksize/2)$$

$$time_{readB_cache} = (48 + 128/2) * (128 - 16) * 128 + (48 + 16 * 128/2) = 1,606,704\ clocks$$

$$time_{read_fullcache} = FIFO\ init\ time + (blocksize/2) * blocksize = 48 + (128/2) * 128 = 8240\ clocks$$

$$time_{writeC} = (FIFO\ init\ time + blocksize/2) * blocksize = (48 + 128/2) * 128 = 14,336\ clocks$$

$$time_{memory} = time_{readA} + time_{readB} + time_{writeC} + overhead = 1,635,376 + overhead$$

$$time_{overall_per_block} = (time_{memory} + time_{block})\ clocks + overhead_{software}$$

$$time_{overall_per_block} = (1,635,376 + 983,040)\ clocks + overhead_{software}$$

$$time_{overall_per_block}\ (in\ sec) = 2,618,416/87,500,000 Hz$$

$$= 0.0299 + overhead_{software}\ seconds$$

Therefore, the overall time to compute the product of two 1024 by 1024 matrices on the FPGA becomes:

$$time_{overall} = (N/blocksize)^3 * time_{overall_per_block} + time_{initialize}$$

$$= (1024/128)^3 * (0.0299 + overhead_{software}) + time_{initialize}$$

$$= 512 * (0.0299 + overhead_{software}) + time_{initialize}$$

$$= 15.3088 + 512 * overhead_{software} + time_{initialize}\ seconds$$

The $time_{initialize}$ becomes a negligible term, but the $overhead_{software}$ is still quite noticeable. The $overhead_{software}$ is small when using a single FPGA, but it is introduced everytime a new block is needed to be loaded onto the FPGA. This term does not increase linearly with the number of FPGAs, because much of the time gets overlapped with itself and computation. This makes it hard to model the actual $overhead_{software}$ for different instances, but after many tests, the overhead for this particular hardware will be modeled as approximately 0.002 seconds per block. The calculation time is not much larger, so this becomes a significant term. The equations now become:

$$overhead_{software} = 0.002\ seconds$$

$$time_{overall_per_block} = 0.0299 + overhead_{software}\ seconds$$

$$\approx 0.0299 + 0.002 \approx 0.0319\ seconds$$

$$time_{overall} = 512 * (0.0319) + time_{initialize}$$

$$\approx 512 * (0.0319) \approx 16.3328\ seconds$$

As mentioned earlier, using multiple FPGAs affects the models slightly, but still achieves almost linear speedup with the number of FPGAs being used making the final equation for computing a 1024 by 1024 matrix multiplication become:

$$time_{overall_parallel} = time_{overall}/(\#\ of\ FPGAs)$$

$$\approx 16.3328/(\#\ of\ FPGAs)\ seconds$$

For this system, a maximum of 4 FPGAs can be used, making the runtime model as approximately:

$$time_{overall_parallel} \approx 16.3328/4 \approx 4.0832\ seconds$$

For double precision the *blocksize* is cut in half, which means that there are more blocks to compute, but each block calculation is faster. Using the same models, the overall runtime becomes:

$$time_{memory} = time_{readA} + time_{readB} + time_{writeC} + overhead = 258,048 + overhead$$

$$time_{overall_per_block} = (time_{memory} + time_{block})\ clocks + overhead_{software}$$

$$time_{overall_per_block} = (258,048 + 217,088)\ clocks + overhead_{software}$$

$$time_{overall_per_block}\ (in\ sec) = 475,136/87,500,000Hz$$

$$= 0.00543 + overhead_{software}\ seconds$$

The $overhead_{software}$ term is now a much more prominent term because the FPGA cannot handle enough computation per block to cover it up. Therefore, the overall time to compute the product of two 1024 by 1024 matrices on the FPGA becomes:

$$time_{overall} = (N/blocksize)^3 * time_{overall_per_block} + time_{initialize}$$

$$\approx (1024/64)^3 * (0.00543 + 0.002)$$

$$\approx 4096 * (0.00743) \approx 30.433\ seconds$$

$$time_{overall_parallel} = time_{overall}/(\#\ of\ FPGAs)$$

$$time_{overall_parallel} \approx 30.433/4 \approx 7.608\ seconds$$

4.5 Results

A number of different results will be presented to verify the runtime models, compare design choices, and show certain attributes of the memory controller on this particular problem (matrix multiplication). Ten trials were run for each type of timed execution and the results were averaged to get a more accurate model than a single test could achieve.

The first order of business to take care of is showing that the application indeed gives the correct results. Figure 4.2 shows the error between varying sizes of matrix multiplications done on both the FPGA and a CPU in double and single precision. In addition, single and double precision are compared together to show how different precisions can affect the overall error of the result.

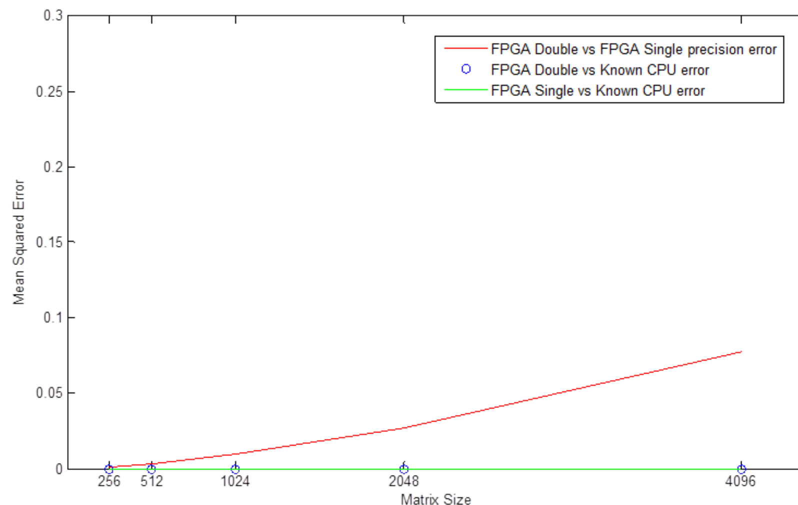

Figure 4.2: Mean Squared Error vs Matrix Size for different precisions of matrix multiplication.

Models of the expected executions times were given earlier in the chapter as well as an example for a 1024x1024 matrix multiplication, but Figure 4.3 shows the actually execution times for different sized matrices. The times are plotted on the same plot as a serial CPU implementation for both single and double precision. The

CPU implementation is a simple IKJ loop structure, but provides a good benchmark to compare against.

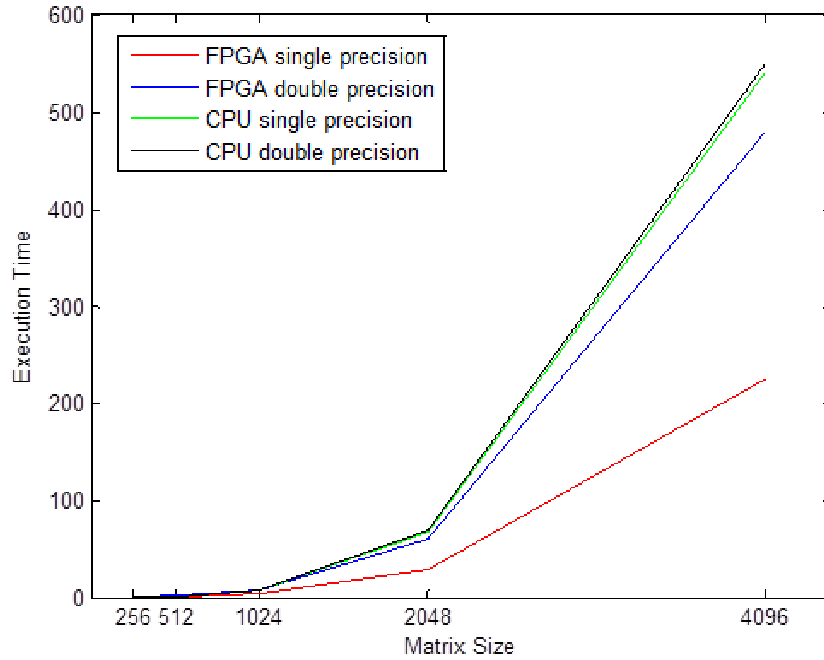

Figure 4.3: Execution Times vs Matrix Size for FPGA (using all 4 FPGAs) and CPU implementations.

Figure 4.4 uses the execution times from Figure 4.3 to show the speedups compared to double precision matrix multiplication on the CPU.

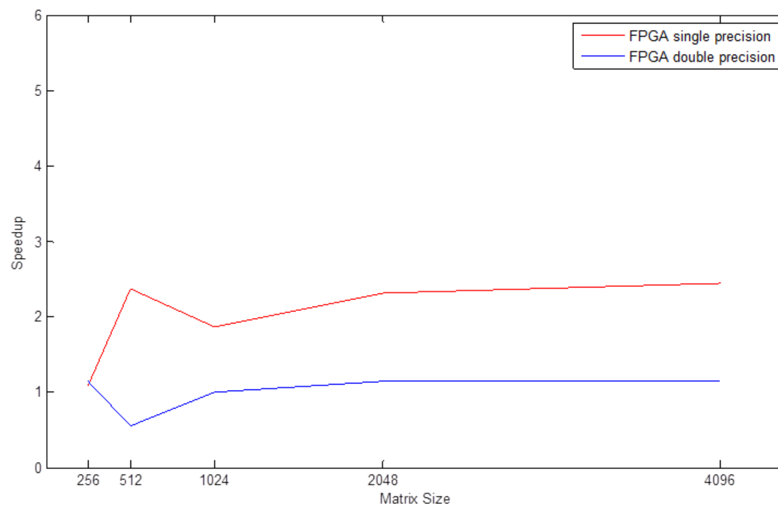

Figure 4.4: Speedup of matrix multiplication on FPGA compared to double precision matrix multiplication performed on CPU.

The effects of caching were described earlier and are a prominent factor in the runtime models. Figure 4.5 shows the effects of using caching and not using caching.

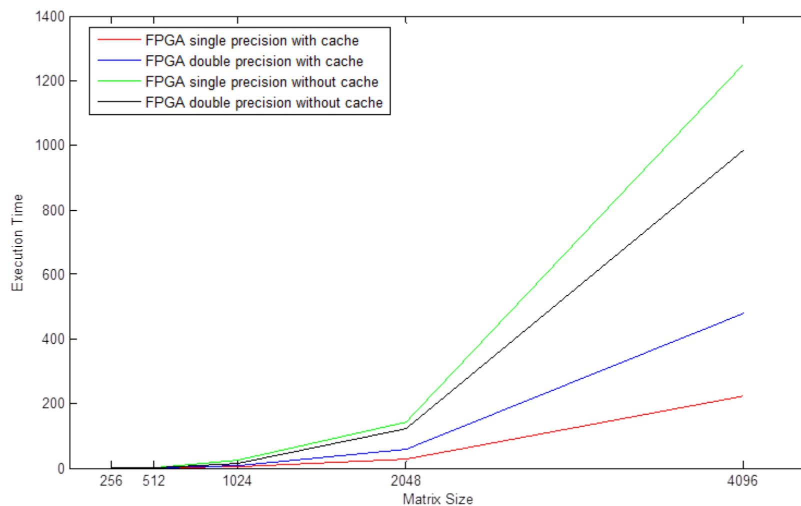

Figure 4.5: Execution Times vs Matrix Size for matrix multiplication on FPGA with caching and no caching.

The effects of caching in terms of speedup over not caching are shown in Figure 4.6.

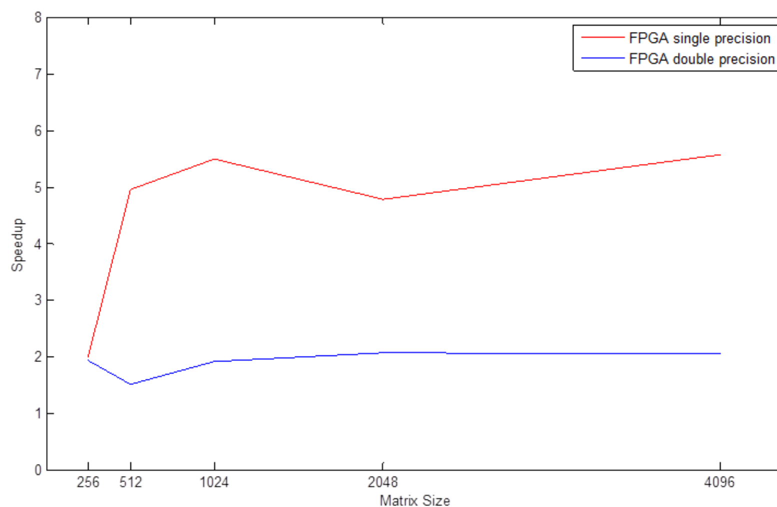

Figure 4.6: Speedup of using caching compared to not using caching on FPGA.

A major benefit of using a coprocessing platform is the ability to add more FPGAs and scale the design. For this particular platform, four FPGAs are connected through the PCIe. For larger applications, a cluster of these platforms would be used, all of which would have four FPGAs. A system like this already exists at the University of Florida called Novo-G [26]. If a design can be scaled to four FPGAs reasonable well, then the next step is scaling the design to multiple nodes through software. Figures 4.7 through 4.10 show how the design scales to four FPGAs on a single node for both single and double precision. It can be concluded that if multiple nodes were used efficiently, the design would also scale to multiple nodes. However, that was beyond the scope of this research.

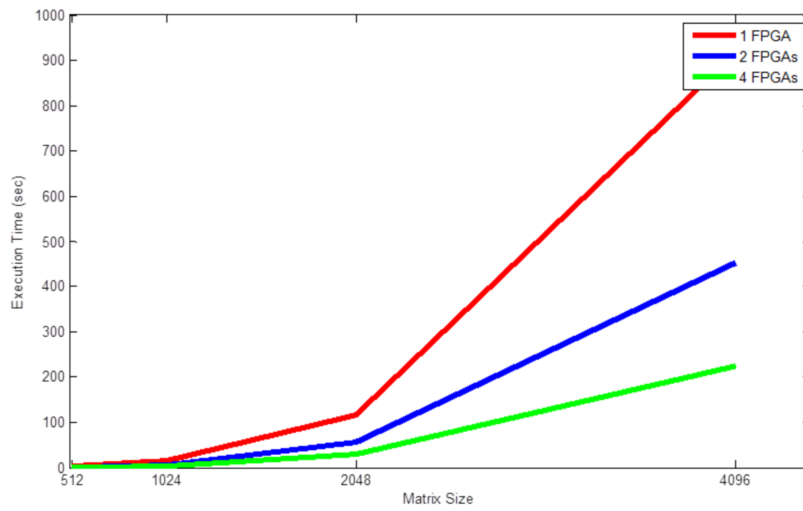

Figure 4.7: Scalability for single precision.

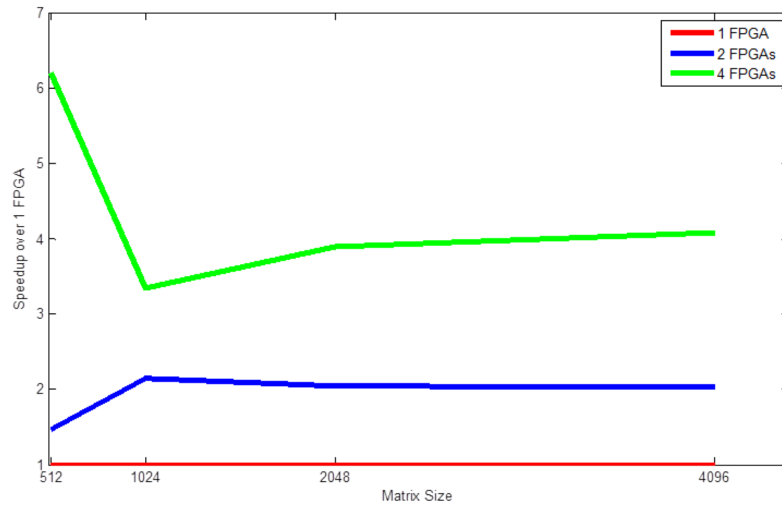

Figure 4.8: Speedup for single precision over using 1 FPGA.

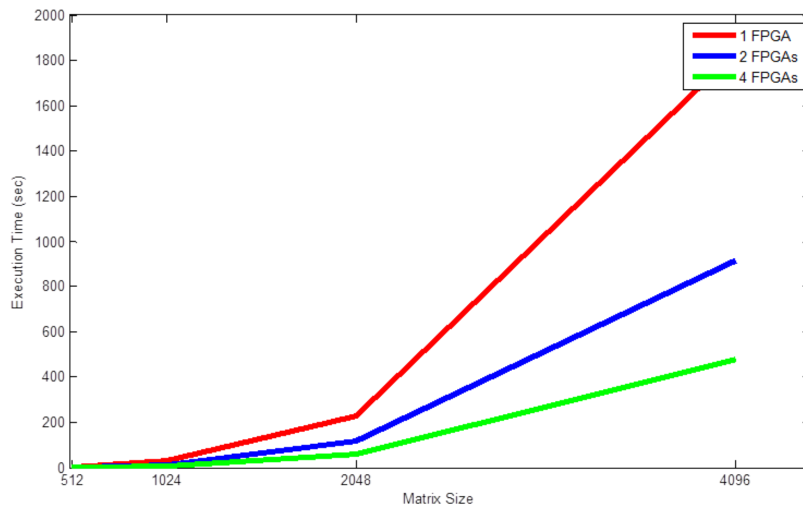

Figure 4.9: Scalability for double precision.

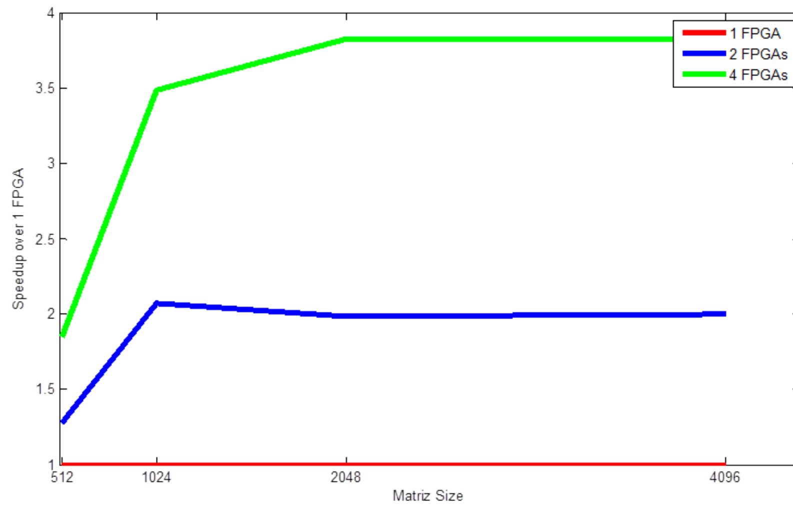

Figure 4.10: Speedup for double precision over using 1 FPGA.

Chapter 5

Discussion

Although the results in the previous chapter behave as expected and show decent performance gains, the matrix multiplication algorithm is not the best target for this type of acceleration. The reason for this is that the overwhelming bottleneck for the design on this particular algorithm is the amount of memory traffic in both hardware and software. For matrix multiplication to be fast, a large number of concurrent floating-point units are required which does not leave enough room for entire matrices to fit into block RAM on the FPGA. Therefore, the much slower SDRAM must be used which bottlenecks the performance. On the contrary, if a smaller number of concurrent floating-point units are used so that matrices can fit into block RAM, the computation becomes the bottleneck. The models show that decreasing the *blocksize* at the expense of less memory traffic is not a good tradeoff, so there is no way to mitigate the bottlenecks for matrix multiplication. Hence, matrix multiplication is not as well suited for this type of system. However, the algorithm was not the focus of this study, so it sufficed to show the effects and correctness of the memory controller.

Algorithms that have less demanding memory constraints compared to their computation times would theoretically fair much better than matrix multiplication for performance gains. Such algorithms would include NP complete problems like the Hamiltonian cycle problem, substring matching, and other similar computationally

intensive problems [21, 22, 23, 24]. The reason for this is because matrix multiplication has a computational complexity of $O(n^3)$, but its memory complexity is $O(n^2)$. The size, n, needs to be large to warrant acceleration for matrix multiplication which means the memory footprint is too large to fit entirely on the FPGA. However, with an algorithm of higher computational complexity, say $O(2^n)$, n does not have to be very large to warrant acceleration. The memory footprint fits entirely into the FPGA and the acceleration has no major bottlenecks. Therefore, the SDRAM is only needed to initially read the values onto the FPGA, and does not need to be continuously referenced.

The performance benefits of using an FPGA as a coprocessor have been thoroughly explored and shown, but there is still another alluring quality that using an FPGA presents. FPGAs are well-documented for their low energy consumption because they operate at slower clock rates [5, 9], while CPUs run at substantially higher clock rates and consume more power. For this reason, FPGAs are targetted by applications that require less power consumption than can be achieved through CPUs.

Chapter 6

Conclusion

The research presented in this thesis discussed the design and implementation of a memory controller for FPGA applications that use floating-point numbers. In particular, the memory controller was designed to be flexible for all floating-point representations, scalable to any number of FPGAs, user-friendly for target applications, and fast for memory transactions that are usually slow. These design objectives were confirmed by performing tests with different parameters applied to a target application, matrix multiplication. In conclusion, the results were excellent for every aspect of the memory controller. However, the performance results could have been much higher if a different target application were used as stated in the Discussion chapter.

Chapter 7

Related Work

The related work that I completed alongside my thesis dealt with computer security. I worked closely with Dr. Gregory D. Peterson and Dr. Nathanael Paul to perform this research and submit a paper to the National Security Innovation Competition. We received 11th place in this competition. The sections below summarize the paper that was submitted for the competition.

Remote identification and authentication are challenging issues often solved by password-based systems. Because adversaries can often guess user passwords, a second step of a login process is used. Today, two-factor authentication is an established method of identity management. Instead of solely relying on authentication through something that you know (e.g., a password), an additional login requirement must be met including (1) something that you have (e.g., a token-generated value) or (2) something that you are (e.g., a fingerprint). Each of these three authentication approaches is independent; a failure in one is independent of another.

These types of two-factor systems have now been largely deployed and were believed to be secure until recent attacks on one of the largest manufacturers in March 2011. At that time, EMCs RSA companys SecureID hardware tokens were compromised, and approximately all 40 million of its tokens needed (or need)

replacement [28]. Many companies use these tokens for secure logins. A company will issue a hardware token for each of its users (e.g., a hardware device that is typically kept on a keychain), and the user will use a password and the tokens computed values for logging into a remote machine. The token will compute and display a new value every 30 seconds. This increases authentication security, because the only devices that can compute the token-generated values are the token and the authentication server to check for valid logins. Our approach mitigates the damage from a potential attack and facilitates simpler, cheaper recovery. While our primary example is the well-known RSA two-factor authentication hardware token system (has 50% of the market with 40 million customers [29]), the architecture is generally applicable to two-factor authentication systems in general. Our system uses custom circuitry to perform token-based authentication, but with additional policies implemented to limit vulnerability to previously employed classes of attacks.

In March 2011, RSA employees received phishing email that contained malware. In this email, the attacker used a zero-day flash vulnerability that was embedded in a Microsoft document [31]. This malware successfully defeated the token-based authentication system, but the specific details of how this happened have not been revealed. A token generates a new token value by computing a function as shown in Figure 7.1. The user supplies a userid, password, PIN code, and token code (i.e., login data), and the authentication server (at right) checks the login data by using the secret key to generate and check the supplied login data.

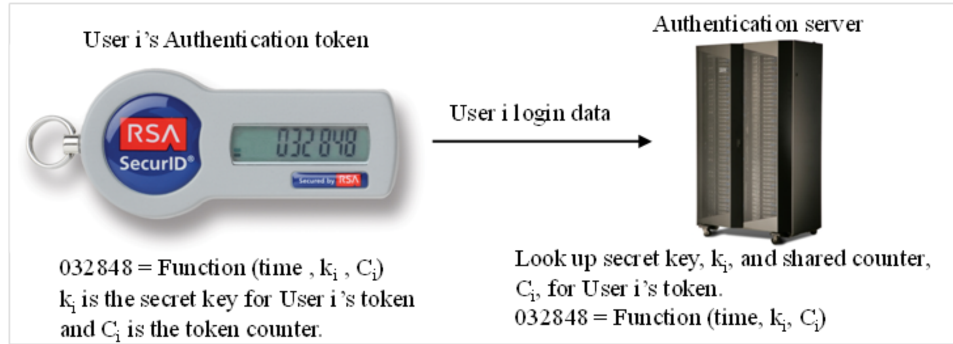

Figure 7.1: Authentication with Traditional Two-factor Hardware Security Tokens. [30]

As long as the secret key is kept secret and authentication servers are synchronized with the user tokens, then the system can authenticate users. Thus, replacing tokens only must be done when secret keys are compromised, or a large amount of future token values are revealed. If the tokens are not replaced, then an adversary could use computed or stored token values to login as someone else if the attacker knew or could break the password. In the March 2011 security breach, L-3 and Lockheed Martin both blame their respective security breaches on this RSA token breach [33]. We must assume that either the secret key for the RSA SecurID tokens were compromised, or a large amount of future token values were compromised.

Our goal in this work is to mitigate attacks where a remote adversary learns login information (i.e., secret key or future token values). We accomplish this through using the token generation server to artificially delay token values to an authentication server. Figure 7.2 shows our changed design for key management and token value management. The authentication server requests a token value whenever a user attempts to login. If a new token value has not been requested for a specified user within the last time period, t, then the new token authentication value is released by the token management device. If a token value has been released for a user within a time period t, then the previous token value is released. To ensure that a remote adversary cannot compromise the key or future token values, the delay for this time

period is enforced in the hardware. In our example RSA system, a reasonable value for t is 30 seconds.

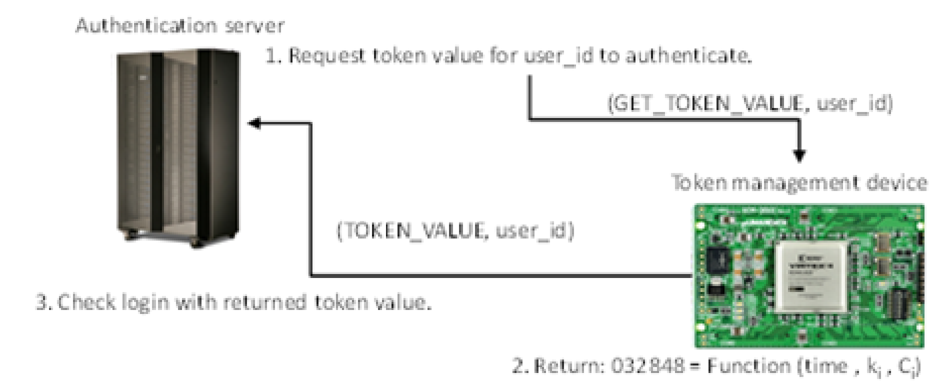

Figure 7.2: Secure Identity Management through Hardware-enforced Security Policies.

Our approach increases operational security in the infrastructure. We use a token server to enforce a policy on token values; this token server is separate from the verifier or authentication server. If we use the token server to repeatedly apply a function to generate new token values, each new value, vi, can be derived as vi = truncate (F (time, ki, Ci)) for 1 i m-1 for some positive m, a monotonically increasing counter Ci, and a key ki [30]. Assuming that F does not repeat (repeating is a possibility in practice), then we can generate an infinitely long sequence of token values. In practice, this is limited to a time-out period of six years in a RSA SecurID SID700 model (some replacement SID700 tokens were issued for six years).

If a remote adversary compromises the authentication server, then the attacker can learn, at most, the current token authentication value. If the remote adversary is able to compromise the token management device, then the built-in hardware delay prohibits learning future token values or the secret key used to generate them. As described, if an adversary were to gain physical access to the token management device, a physical hardware compromise could still compromise the distributed hardware security tokens.

To demonstrate a proposed protection scheme against physical hardware compromise, we assume that each token uses a unique key to generate token values for one year (the time period is arbitrary). For keys used in year two, we encrypt them until they are needed. A hardware compromise would then yield, at most, one years worth of token values (i.e., the keys used to generate those token values). The encryption keys used to encrypt the token-generating keys can be split using a threshold cryptographic scheme. For example, if each year of a tokens lifespan was encrypted with a key split into multiple parts, then a collusion between the holders of these key parts would be needed for reassembly. Once these keys were reassembled, the token-generating keys could be decrypted and used for each subsequent year.

The parties holding the future keys to unlock later authentication codes could involve multiple parties at the manufacturer, or it could involve parties at user organizations. With these added parties involved in the authentication process, the threshold cryptographic storage of keys adds additional complexity. Key parts could be mislabeled (e.g., year 2 could be switched with year 3) and extra management is needed to reassemble keys. However, this will be an attractive solution, even if only done for some subset of the user population. Given that these token authentication schemes are used to defend access to critical data, involving multiple parties that include the token manufacturer, the users, and government officials help further protect future token values by requiring collusion across organizations for key assembly.

With this new approach, recovery is now made possible. Assume that a remote adversary gains physical access to a token management device. Once this is detected, all token values that would be generated for the next calendar year are compromised (i.e., the keys used to generate those values have been compromised). If we can force tokens to switch to a new token-generating key early, then this avoids great costs. To do this, we augment current tokens with a new feature that can reset the token-generating key that also synchronizes with the token management device. One

possible way of doing this is through a hardware button where a user presses the button according to some specified sequence to switch to a new key.

This architecture now enables new security guarantees. If an attacker were to remotely compromise a device that receives a token value from a token generating device, the attacker can only read a value every t time units. The hardware delay cannot be circumvented remotely. This increases two-factor authentication security by moving the key to a location that should only be compromised under physical access (assuming that predicting future token values is computationally infeasible without the key used to generate those values). We can quantify how many token values an attacker can have obtained by computing how many values have been released from the time of compromise. For example, if a compromise was a result of a particular email, we know that the earliest point of compromise could not have happened before the first SPAM email was delivered. To be safe, a new token-generating key can be used by switching to a future time period (e.g., an early switch to year ks token-generating key is made before the end of year k-1). This is accomplished through the reassembling of the token-generation key.

In order to demonstrate our methodology, the backend of the design was implemented on an FPGA. The platform was the same platformed used for the rest of the research. Essentially, the FPGA receives a candidate token, a userID, and a time from software. In order to check if the candidate token is correct at the current time, the user ID and time are used to reconstruct the expected token. If the candidate token matches the expected token, then the user is successfully authenticated and is able to login. The prototype enforces our policy on token timing by not updating the expected token for a given user until the 30-second window has expired. Figure 7.3 shows the design of the prototype.

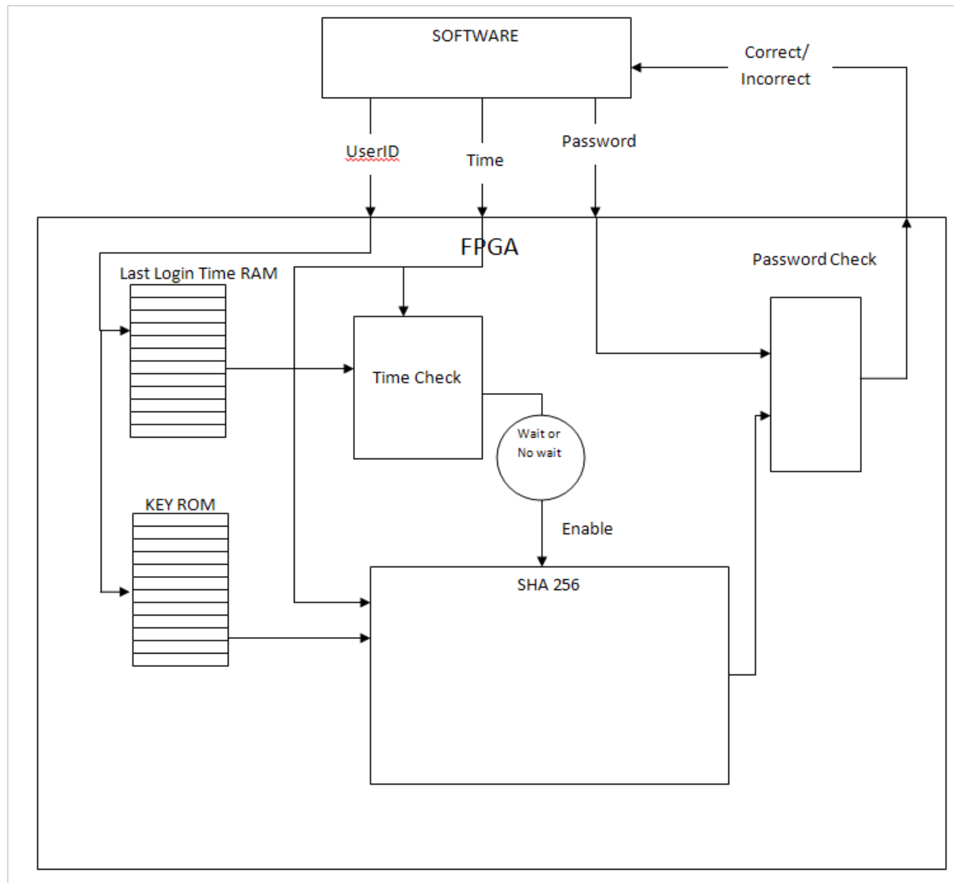

Figure 7.3: Design of Prototype.

Bibliography

Bibliography

[1] Pong P. Chu, ”FPGA Prototyping by VHDL Examples: Xilinx Spartan-3 Version”, *John Wiley & Sons, Inc.*, 2008.

[2] Hartmut F.-W. Sadrozinski and Jinyuan Wu, ”Applications of Field-Programmable Gate Arrays in Scientific Research”, *Taylor & Francis*, 2010. 1

[3] Levinson H. Simmle and Reinhard Manner, ”Multitasking on FPGA Coprocessors”, *FPL '00 Proceedings of the The Roadmap to Reconfigurable Computing, 10th International Workshop on Field-Programmable Logic and Applications*, 2000, pp. 121–130. 1

[4] G. Govindu, L. Zhuo, S. Choi, and V. Prasanna. ”Analysis of High-performance Floating-point Arithmetic on FPGAs”. *In Proceedings of the 18th International Parallel and Distributed Processing Symposium (IPDPS04)*, pages 149156, April 2004.

[5] J. Jang, S. Choi, and V. K. Prasanna, ”Energy-Efficient Matrix Multiplication on FPGAs”. *In Proceedings of the 12th International Workshop on Field Programmable Logic and Application (FPL 2002)*, pages 534544. LNCS 2438, August 2002. 45

[6] J. Jang, S. Choi, and V. K. Prasanna. ”Area and Time Efficient Implementations of Matrix Multiplication on FPGAs”. *In Proceedings of the IEEE International Conference on Field-Programmable Technology (FPT 2002)*, pages 93100, December 2002.

[7] G. Lienhart, A. Kugel, and R. Manner. "Using Floating-Point Arithmetic on FPGAs to Accelerate Scientific N-Body Simulations". *In Proceedings of the IEEE Symposium on Field-Programmable Custom Computing machines (FCCM 2002)*, pages 182191, April 2002.

[8] W. B. Ligon III, S. McMillan, G. Monn, K. Schoonover, F. Stivers, and K. D. Underwood. "A Re-evaluation of the Practicality of Floating-Point Operations on FPGAs". *In Proceedings of the IEEE Symposium on Field-Programmable Custom Computing machines (FCCM 1998)*, pages 206215, April 1998.

[9] R. Scrofano, S. Choi, and V. K. Prasanna. "Energy Efficiency of FPGAs and Programmable Processors for Matrix Multiplication". *In Proceedings of the IEEE International Conference on Field-Programmable Technology (FPT 2002)*, pages 422425, December 2002. 45

[10] GiDEL, "Proc API", *Data Book*, 2012. 4

[11] GiDEL, "ProcWizard", *User's Manual Version 8.8*, 2010. 3

[12] GiDEL, "ProcMultiport IP SDRAM Controller", *User's Guide*, 2011. viii, 4, 7, 8

[13] Altera, "Floating-Point Megafunctions", *User Guide*, 2011.

[14] Altera, "Accelerating High-Performance Computing with FPGAs", *Altera White Paper*, 2007. 1

[15] Lattice Semiconductor, "Developing High-speed Memory Interfaces: The LatticeSCM FPGA Advantage", *A Lattice Semiconductor White Paper*, February 2006.

[16] Ashley Brown, Paul Kelly, and Wayne Luk, "Profiling floating point value ranges for reconfigurable implementation", *Proceedings of the 1st HiPEAC Workshop on Reconfigurable Computing*, Ghent, Belgium, January 2007. 1

[17] Haru Shimada and Akinori Kanasugi, "A Dynamically Reconfigurable Arithmetic Circuit for Complex Number and Double Precision Number", *World Academy of Science, Engineering and Technology*, Vol. 54, 2009.

[18] Michael Lam, Jeffrey Hollingsworth, and Akinori Kanasugi, "Dynamic Floating-Point Cancellation Detection", *First International Workshop on High-performance Infrastructure for Scalable Tools*, Tuscon AZ, June 2011.

[19] Nirav Dave , Kermin Fleming, Myron King, Michael Pellauer, and Muralidaran Vijayaraghavan, "Hardware Acceleration of Matrix Multiplication on a Xilinx FPGA", Computer Science and Artificial Intelligence Lab, Massachusetts Institute of Technology.

[20] P. M. Zhong, Martonosi, P. Ashar, and S. Malik, Using Configurable Computing to Accelerate Boolean Satisfiability, *IEEE Transactions on CAD of Integrated Circuits and Systems*, vol. 18, No. 6, June 1999.

[21] K. B. Kent, S. Van Schaick, J. E. Rice, and P. A. Evans, "Hardware-based implementation of the common approximate substring algorithm, *Digital System Design, 2005. Proceedings. 8th Euromicro Conference*, September 2005. 45

[22] K. B. Kent and M. Serra, Using FPGAs to Solve the Hamiltonian Cycle Problem, *International Symposium on Circuits and Systems (ISCAS) 2003*, May 2003. 45

[23] K. B. Kent and M. Serra, Using Instance-Specific Circuits to Compute Autocorrelation Coefficients, *First Northeast Workshop on Circuits and Systems, 2003*. 45

[24] K. B. Kent, B. C. Iaderoza, and M. Serra, "Codesign of a Computationally Intensive Problem in GF(3)", *Rapid Systems Prototyping, 2007. RSP 2007. 18th IEEE/IFIP International Workshop*, May 2007. 45

[25] Manuel Jimenez, Nayda Santiago, and Diane Rover, "Development of a Scalable FPGA-Based Floating Point Multiplier", December 1995.

[26] *Novo-G: Adaptively Custom Research Supercomputer*. Retrieved June 7, 2012 from http://www.chrec.org/facilities.html. 41

[27] Battle.net Authenticator. Blizzard Entertainment. Available at http://us.blizzard.com/store/search.xml?q=authenticator.

[28] Siobhan Gorman and Ghara Tibken. "Security Tokens Take Hit". *The Wall Street Journal*. June 7, 2011. 48

[29] Rachael King. "EMC's RSA Security Breach May Cost Bank Customers 100 Million". Bloomberg. Available at http://www.bloomberg.com/news/2011-06-08/emc-s-rsa-security-breach-may-cost-bank-customers-100-million.html. 48

[30] D. M'Raihi, S. Machani, M. Pei, and J. Rydell. "TOTP: Time-Based One-Time Password Algorithm". *Internet Engineering Task Force (IETF) Request for Comments 6238*, May 2011. ix, 49, 50

[31] Uri Rivner. "Anatomy of an Attack." Speaking of Security: The Official RSA Blog and Podcast. Available at http://blogs.rsa.com/rivner/anatomy-of-an-attack. 48

[32] Keith Stuart. "PlayStation hack: network will be back in days, says Sony." theguardian. April 28, 2011. Available at http://www.guardian.co.uk/technology/gamesblog/2011/apr/28/playstation-hack-network-sony-psn.

[33] Jaikumar Vijayan. "Cyberattacks fuel concerns about RSA SecurID breach." *Computerworld*. June 1, 2011. Available at http://www.computerworld.com/s/article/9217216/Cyberattacks_fuel_concerns_about_RSA_SecurID_breach. 49

Vita

Bryan Jacob Hunter was born in Nashville, TN on 3 March 1988. He graduated from Mt. Juliet High School in 2006 where he went on to the University of Tennessee in Knoxville, TN. He received his Bachelor of Science in Electrical Engineering in May 2010. He continued his education at UTK where he is currently pursuing his Master of Science degree in Computer Engineering.